

UCSF

UC San Francisco Previously Published Works

Title

Magnetic Resonance Measurement of Turbulent Kinetic Energy for the Estimation of Irreversible Pressure Loss in Aortic Stenosis

Permalink

<https://escholarship.org/uc/item/7cg784wj>

Journal

JACC Cardiovascular Imaging, 6(1)

ISSN

1936-878X

Authors

Dyverfeldt, Petter

Hope, Michael D

Tseng, Elaine E

et al.

Publication Date

2013

DOI

10.1016/j.jcmg.2012.07.017

Peer reviewed



Published in final edited form as:

*JACC Cardiovasc Imaging*. 2013 January ; 6(1): 64–71. doi:10.1016/j.jcmg.2012.07.017.

## Magnetic Resonance Measurement of Turbulent Kinetic Energy for the Estimation of Irreversible Pressure Loss in Aortic Stenosis

Petter Dyverfeldt, PHD<sup>\*</sup>, Michael D. Hope, MD<sup>\*</sup>, Elaine E. Tseng, MD<sup>†,‡</sup>, and David Saloner, PHD<sup>\*,†,‡</sup>

<sup>\*</sup>Department of Radiology and Biomedical Imaging, University of California San Francisco, San Francisco, California

<sup>†</sup>Department of Surgery, University of California San Francisco, San Francisco, California

<sup>‡</sup>Veterans Affairs Medical Center, San Francisco, California

### Abstract

**OBJECTIVES**—The authors sought to measure the turbulent kinetic energy (TKE) in the ascending aorta of patients with aortic stenosis and to assess its relationship to irreversible pressure loss.

**BACKGROUND**—Irreversible pressure loss caused by energy dissipation in post-stenotic flow is an important determinant of the hemodynamic significance of aortic stenosis. The simplified Bernoulli equation used to estimate pressure gradients often misclassifies the ventricular overload caused by aortic stenosis. The current gold standard for estimation of irreversible pressure loss is catheterization, but this method is rarely used due to its invasiveness. Post-stenotic pressure loss is largely caused by dissipation of turbulent kinetic energy into heat. Recent developments in magnetic resonance flow imaging permit noninvasive estimation of TKE.

**METHODS**—The study was approved by the local ethics review board and all subjects gave written informed consent. Three-dimensional cine magnetic resonance flow imaging was used to measure TKE in 18 subjects (4 normal volunteers, 14 patients with aortic stenosis with and without dilation). For each subject, the peak total TKE in the ascending aorta was compared with a pressure loss index. The pressure loss index was based on a previously validated theory relating pressure loss to measures obtainable by echocardiography.

**RESULTS**—The total TKE did not appear to be related to global flow patterns visualized based on magnetic resonance-measured velocity fields. The TKE was significantly higher in patients with aortic stenosis than in normal volunteers ( $p < 0.001$ ). The peak total TKE in the ascending aorta was strongly correlated to index pressure loss ( $R^2 = 0.91$ ).

**CONCLUSIONS**—Peak total TKE in the ascending aorta correlated strongly with irreversible pressure loss estimated by a well-established method. Direct measurement of TKE by magnetic resonance flow imaging may, with further validation, be used to estimate irreversible pressure loss in aortic stenosis.

## Keywords

aortic stenosis; magnetic resonance imaging; pressure loss; transvalvular pressure gradient; turbulent kinetic energy

Noninvasive determination of irreversible pressure loss has long been a goal of cardiovascular imaging. Irreversible pressure loss caused by energy dissipation in post-stenotic flow is an important marker of the hemodynamic significance of aortic stenosis. The left ventricle has to respond with increased work to overcome this loss of mechanical energy, resulting in increased stress on the myocardium.

The true irreversible pressure loss (net transvalvular pressure gradient,  $TPG_{net}$ ) is currently best estimated by simultaneous catheter-based pressure recordings in the left ventricle and the distal ascending aorta. However, this procedure is invasive and therefore not used routinely. The current method of choice in the clinical assessment of transvalvular pressure differences is noninvasive echocardiography. Based on an estimation of the peak velocity in the vena contracta ( $v_{VC}$ ) of the post-stenotic flow jet, the maximum drop in (static) pressure across the valve (maximum transvalvular pressure gradient,  $TPG_{max}$ ) is estimated by the simplified Bernoulli equation in combination with the assumption that  $v_{VC}$  is much greater than the flow velocity in the left ventricle (1):

$$TPG_{max} = 4v_{VC}^2 [\text{mmHg}] \quad [1]$$

The degree to which  $TPG_{max}$  represents  $TPG_{net}$  depends on the amount of kinetic energy that is dissipated distal to the vena contracta, where the flow transitions from a laminar to a turbulent state during systole. A portion of the kinetic energy that is not dissipated is converted into static pressure, resulting in so-called pressure recovery (2–9). Due to pressure recovery,  $TPG_{max}$  overestimates  $TPG_{net}$  and the increased workload imposed on the left ventricle by pressure loss (2–6). For example, a recent study reported that more than 20% of  $TPG_{max}$  was recovered in 16.8% of a large patient population (6). The clinical implications of the inability of echocardiography to account for pressure recovery are frequently debated (7–9).

A noninvasive approach to the estimation of true irreversible pressure loss could refine the diagnosis of aortic stenosis. Consequently, several investigators have proposed indexes aimed at addressing the discrepancy between  $TPG_{max}$  and  $TPG_{net}$  based on data that can be obtained by noninvasive imaging (8,10–13). These indexes typically take into account the severity of the sudden expansion that occurs between the valve and the ascending aorta, which is known to promote transition to nonlaminar flow. Despite being implicit and based on assumptions about standardized transvalvular flow patterns, such approaches have been shown to permit noninvasive estimation of irreversible pressure loss in in vitro experiments, animal models, and specific patient groups (4,11,13,14). For example, Garcia et al. (12,13) (see also Akins et al. [8]) added an energy loss term to the Bernoulli equation to account for its inability to describe pressure losses and combined that with the momentum equation. They noted that irreversible pressure loss depends on the flow rate ( $Q$ ) and that it increases with decreasing vena contracta area ( $A_{VC}$ ) and with increasing aortic area ( $A_{Ao}$ ). When combining their results for  $TPG_{net}$  with the widely used approximation that  $v_{VC}$  is much greater than the flow velocity in the left ventricle in patients with aortic stenosis (Equation 1), the following relationship is obtained (12,13):

$$\frac{\text{TPG}_{\text{net}}}{\text{TPG}_{\text{max}}} = \left(1 - \frac{A_{\text{vc}}}{A_{\text{Ao}}}\right)^2 \quad [2]$$

By also taking the flow rate dependency into account (12), this can be written as a pressure loss index (iPL) that can be used in patients with varying flow rates:

$$\text{iPL} = Q \frac{\text{TPG}_{\text{net}}}{\text{TPG}_{\text{max}}} = Q \left(1 - \frac{A_{\text{vc}}}{A_{\text{Ao}}}\right)^2 \quad [3]$$

Direct measurement of the flow effects responsible for irreversible pressure loss is now possible with magnetic resonance (MR) imaging. This potentially offers a more appealing way than iPLs to correct for gross discrepancies between echocardiography and catheter-based pressure gradients. In the transitionally turbulent flow regime distal to the vena contracta, the kinetic energy can be decomposed into 2 parts: the mean kinetic energy and the turbulent kinetic energy (TKE). The dominant cause of irreversible pressure loss in clinically relevant aortic stenosis is viscous dissipation of TKE into heat (15).

Recent developments in phase-contrast magnetic resonance imaging (PC-MRI) permit noninvasive estimation of TKE (16,17). There is an important conceptual difference between PC-MRI velocity and TKE mapping. Whereas conventional PC-MRI velocity mapping estimates mean velocities based on the phase-difference between 2 complex-valued MR signals acquired with different motion sensitivity, TKE estimation is achieved by exploiting the fact that the relationship in signal amplitude between 2 such signals is related to the distribution of velocities within a voxel (16). The amount of motion sensitivity used in TKE mapping is preferably chosen to obtain about 50% signal drop at the TKE values of interest (18,19). The PC-MRI TKE mapping technique has been successfully validated against particle image velocimetry, as well as computational fluid dynamics, both in vitro and in vivo (18–21). The feasibility of the technique for time-resolved 3-dimensional (i.e., 4-dimensional [4D]) measurements of TKE fields in the human cardio-vascular system has been demonstrated in a wide range of applications (17,22).

The aim of this study was to characterize TKE in the ascending aorta of patients with aortic stenosis and to assess the relationship between TKE and irreversible pressure loss. TKE measurements were compared with previously validated pressure loss indexes that can be obtained by noninvasive imaging.

## METHODS

### Subjects

The study was approved by the local ethics review board, and all subjects gave written informed consent. A total of 18 subjects (14 aortic stenosis patients with/without ascending aortic dilation, 4 normal volunteers) were enrolled (Table 1) (23). All subjects underwent 4D PC-MRI flow imaging, and the patients had a clinical computed tomography and echocardiography investigation done within 10 and 7 weeks, respectively, of the MR study. A broad range of aortic stenoses was represented in the study.

### MR flow imaging and estimation of TKE

For the assessment of TKE, 4D PC-MRI data were acquired during free breathing on a clinical 1.5-T MR scanner (Siemens Avanto, Siemens, Erlangen, Germany) using a

prospectively cardiac-gated gradient echo sequence with asymmetrical 4-point motion encoding, where the latter enables TKE estimation (16). Respiratory effects were suppressed by using navigator gating with a 7-mm acceptance window. Other imaging parameters included TR/TE: 4.3 to 4.4/2.7 to 2.9 ms, flip angle: 8°, k-space segmentation factor: 2, parallel imaging reduction factor: 2. The 3-dimensional field-of-view (240 to 360 × 240 to 360 × 55 to 80 mm<sup>3</sup>) and matrix size (96 to 144 × 96 to 144 × 22 to 32) was adjusted depending on each subject's anatomy to cover the thoracic aorta with a sagittal-oblique slab orientation while maintaining an isotropic voxel size of 2.5 × 2.5 × 2.5 mm<sup>3</sup>. Total scan time was about 10 to 25 min, depending on the navigator efficiency. On the basis of previous in vivo studies with MR TKE mapping, we anticipated peak TKE values of about 1,200 to 1,600 J/m<sup>3</sup> in the patients studied here. Assuming isotropic turbulence, a velocity encoding (VENC) value of 280 cm/s provides optimum TKE sensitivity at TKE ~1,400 J/m<sup>3</sup> (18). TKE values considerably higher than the optimal value are underestimated due to the Rician distribution of MR magnitude data (18). Consequently, the VENC was set to 280 cm/s in the patients so as to obtain good TKE sensitivity and avoid underestimation. The fact that this VENC setting resulted in aliasing of the highest velocities in some of the patients was not a concern as the TKE is based on signal amplitude and is thus insensitive to such effects. A VENC of 200 cm/s was used in the normal volunteers.

Velocity fields were reconstructed on the scanner using standard phase-difference algorithms and were corrected off-line for background phase offsets and velocity aliasing when needed. Offline reconstruction using a MATLAB script (MathWorks, Natick, Massachusetts) written in-house was used to reconstruct the magnitude images of the individual flow encoding segments as needed to obtain the TKE (16,17).

The TKE per unit volume is defined as (24):

$$\text{TKE} = \frac{1}{2} \rho \sum_{i=1}^3 \sigma_i^2 [\text{Jm}^{-3}] \quad [4]$$

where  $\rho$  is the fluid density and  $\sigma_i$  is the turbulence intensity (intensity of velocity fluctuations) in 3 mutually perpendicular directions  $i$ . A 3-directional PC-MRI measurement carried out with asymmetric 4-point motion encoding, as done here, provides  $\sigma_i$  in 3 mutually perpendicular directions, thus enabling the calculation of TKE (17). The relationship used to compute  $\sigma_i$  appears as (16,25):

$$\sigma_i = \frac{1}{k_v} \sqrt{2 \left( \frac{|S|}{|S_i|} \right)} \quad [5]$$

where  $|S|$  and  $|S_i|$  denote the amplitude of a complex-valued MR signal acquired with zero first-order motion sensitivity and motion sensitivity in direction  $i$ , respectively.  $k_v$  (i.e.,  $\pi/\text{VENC}$ ) describes the net motion sensitivity. The fluid density was assumed to be 1.060 kg/m<sup>3</sup>.

### Estimation of pressure loss

The iPL described in Equation 3 was used to assess the relationship between TKE and irreversible pressure loss. Each variable of the pressure loss index was measured with the most reliable modality available: flow rate with PC-MRI, aortic valve area with echocardiography, and aortic diameter with computed tomography (26–28). Aortic area was measured at the site of the sinotubular junction, as recommended (6,13). In the normal volunteers, aortic area was estimated from the MR data. Flow rate was measured at peak flow systole.

## Data analysis

Using commercially available software (EnSight 9.2, CEI, Apex, North Carolina), a protocol was defined for visual inspection of velocity and TKE fields in the ascending aorta of each subject. Post-stenotic mean velocity fields were assessed by generating short streamlines throughout the entire ascending aorta in each time frame. Streamlines represent instantaneous velocity fields and are always tangent to the direction of the velocity vector. Visualization of the spatiotemporal distribution of TKE was achieved by volume rendering of the TKE data in the ascending aorta at each time frame.

The total TKE in the ascending aorta was calculated at each time frame by integrating the TKE over the aortic segment spanning from the aortic valve to a standardized level midway between the brachiocephalic and left common carotid arteries where velocity fluctuations had dampened out and TKE was low in all subjects. Geometrical constraints were obtained by manual segmentation of the 4D PC-MRI data. Plots of total TKE over time were generated for each subject.

Simple linear regression was used to assess the relationship between TKE and irreversible pressure loss with total peak systolic TKE as the independent variable and iPL as the dependent variable. A 2-sample *t* test was performed to assess whether TKE in the patients was higher than in the normal volunteers.

## RESULTS

Plots of the total TKE in the ascending aorta of each subject are shown in Figure 1. Peak total TKE in the patients (TKE = 3 to 52 mJ) was higher than in the normal volunteers (TKE < 3 mJ),  $p < 0.001$ . The presentation of hemodynamics was consistent in all normal volunteers but notably diverse in the patients. Peak total TKE occurred post-peak systole, and the primary regions of elevated TKE appeared to be located in regions of flow jet deceleration and wall detachment. The total TKE did not appear to be related to global flow patterns. Figure 2 shows data for 1 normal volunteer and 3 patients that exemplify the degree of diversity. The patients shown in Figures 2B (Patient #9,  $Q_{\text{peak}} = 420$  ml/s) and 2D (Patient #7,  $Q_{\text{peak}} = 750$  ml/s) both have eccentric flow directed towards the outer wall of the ascending aorta accompanied by vertically recirculating flow. Peak total TKE in these subjects was 13 and 38 mJ, respectively. The patients shown in Figures 2C (Patient #5,  $Q_{\text{peak}} = 920$  ml/s) and 2D, by contrast, have similar peak total TKE (40 vs 38 mJ) but markedly different flow patterns.

The peak total TKE in the ascending aorta was strongly correlated with iPL (Fig. 3). The estimated regression function was  $\text{iPL} = 23.2 + 14.9 \times \text{TKE}_{\text{total}}$ ,  $R^2 = 0.91$ . The intercept was not significantly different from zero. The slope was significantly different from zero,  $p < 0.001$ . For patients only,  $R^2$  was 0.81.

## DISCUSSION

The main finding of this study is that noninvasive MR flow imaging can be used to estimate irreversible pressure loss in the ascending aorta. The strong relationship between TKE as measured by noninvasive MR flow imaging and iPL (Fig. 3) suggests that for aortic stenosis with a given  $\text{TPG}_{\text{max}}$  and flow rate, the amount of TKE reflects the amount of energy dissipation and thus the hemodynamic significance of the stenosis. This accords well with theoretical fluid mechanics considerations of pressure loss in aortic stenosis (8,15).

The finding that TKE reflects irreversible pressure loss has potential clinical implications. Although accessibility and cost will likely keep echocardiography as the first-line

noninvasive method for the evaluation of aortic stenosis, pressure gradient estimation based on the simplified Bernoulli equation (Equation 1) often misclassifies the ventricular overload caused by aortic stenosis (2–6). Echocardiography-based methods for estimation of irreversible energy or pressure loss have shown promising results but are not yet used routinely (27). These methods are limited by assumptions about standardized flow patterns and are reportedly confounded by the presence of eccentric flow (29,30). Variability related to the echocardiography measurement of aortic diameter may be another limiting factor (27). Catheterization-based pressure measurements are invasive and not used routinely. TKE measurements by MR flow imaging are noninvasive and do not rely on assumptions about standardized flow patterns. By combining Equation 3 with the estimated regression function,  $TPG_{net}$  can be calculated from the total TKE according to  $TPG_{net} = TPG_{max} / Q^2 (23.2 + 14.9 TKE_{total})$  [mm Hg]. In this way, TKE data could be incorporated into the clinical evaluation of aortic stenosis and be directly compared to pressure estimates obtained with echocardiography and catheterization.

This new approach for the direct measurement of the flow effects responsible for pressure loss is relatively simple to perform. The only processing step needed to obtain the total TKE (Figs. 1 and 3) is segmentation of the ascending aorta. In the present study, segmentation was done manually, and processing time was 5 min per patient. Automatic segmentation of 4D PC-MRI is expected to be realized in the near future (31). Estimation of TKE requires measurements of turbulence intensity in 3 mutually perpendicular directions (Equation 4), and the calculation of total TKE in the aorta additionally requires volumetric TKE measurements. Currently, MR imaging is the only method that can be used in vivo that is capable of obtaining such comprehensive data on energy-dissipating flow effects. Invasive hot film/wire anemometry and perivascular Doppler ultrasound have the ability to provide some information on turbulence intensity in vivo (32,33). Noninvasive echocardiography methods have also been proposed and may be able to contribute with first-order estimations of nonlaminar flow effects associated with aortic stenosis (34,35).

Others have shown that relative pressure fields can be computed from 4D PC-MRI velocity data (36,37). Although this is valuable for the investigation of normal human cardiovascular pressure dynamics, the underlying equations (Navier-Stokes equations) use only the mean velocity, or acceleration, field as input and do not take energy dissipation into account. By extending TKE measurements to obtain the so-called turbulence stress tensor, which is the subject of ongoing research (38), pressure calculations may be extended to take energy dissipation into account. This would further enhance the noninvasive imaging armamentarium for in-depth investigations of energy-dissipating flows and potentially enable noninvasive pressure field mapping in aortic stenosis.

### Study limitations

A limitation of this study was the lack of a true reference for transvalvular pressure loss. Simultaneous recordings of pressure in the left ventricle and the distal ascending aorta using high-fidelity pressure catheters is currently considered the gold standard for the estimation of transvalvular pressure loss. Although the approach used here for calculation of the pressure loss index has previously been validated against catheter-based methods and is well established (6–8,12,13), more studies are needed to further assess the relationship between TKE and irreversible pressure loss. Catheter-measured pressure loss was available in 1 of our patients. This patient had a measured  $TPG_{net}/TPG_{max}$  ratio of 0.89, which corresponded well to the estimated  $TPG_{net}/TPG_{max}$  ratio of 0.85. A limitation of the 4D PC-MRI technique used here is that relatively long scan times are needed to obtain adequate spatiotemporal resolution and coverage. However, advances in accelerated 4D PC-MRI indicate that total scan times of <10 min are likely in the near future (39,40).

## CONCLUSIONS

This study used a novel MR flow imaging method to measure the total TKE in the ascending aorta of patients with aortic stenosis and assessed the relationship between TKE and irreversible pressure loss. Peak total TKE in the ascending aorta correlated strongly with a iPL calculated based on well-established methods. Direct measurement of TKE may, with further validation, be used to estimate irreversible pressure loss in aortic stenosis.

## Acknowledgments

The authors thank Tino Ebbers for sharing his group's post-processing tools.

Dr. Dyverfeldt was supported by the Fulbright Commission, the Swedish Heart-Lung Foundation, and the Swedish Brain Foundation. Dr. Hope was supported by an RSNA Research Scholar grant. Dr. Tseng was supported by a grant from the Coulter Foundation and an American Heart Association Grant-in-Aid, administered by the Northern California Institute for Research and Education using resources from the San Francisco VA Medical Center. Dr. Saloner was supported by a VA MERIT review grant and NIH grant NS 059944.

## ABBREVIATIONS AND ACRONYMS

<b>4D</b>	4-dimensional (3 spatial dimensions + time)
<b>iPL</b>	pressure loss index
<b>MR</b>	magnetic resonance
<b>PC-MRI</b>	phase-contrast magnetic resonance imaging
<b>TKE</b>	turbulent kinetic energy
<b>TPG</b>	transvalvular pressure gradient
<b>VENC</b>	velocity encoding

## REFERENCES

1. Hatle L, Angelsen BA, Tromsdal A. Non-invasive assessment of aortic stenosis by Doppler ultrasound. *Br Heart J*. 1980; 43:284–292. [PubMed: 7437175]
2. Ohlsson J, Wranne B. Noninvasive assessment of valve area in patients with aortic stenosis. *J Am Coll Cardiol*. 1986; 7:501–508. [PubMed: 3950229]
3. Laskey WK, Kussmaul WG. Pressure recovery in aortic valve stenosis. *Circulation*. 1994; 89:116–121. [PubMed: 8281636]
4. Schobel WA, Voelker W, Haase KK, Karsch KR. Extent, determinants and clinical importance of pressure recovery in patients with aortic valve stenosis. *Eur Heart J*. 1999; 20:1355–1363. [PubMed: 10462470]
5. Gjørtsson P, Caidahl K, Svensson G, Wallentin I, Bech-Hanssen O. Important pressure recovery in patients with aortic stenosis and high Doppler gradients. *Am J Cardiol*. 2001; 88:139–144. [PubMed: 11448410]
6. Bahlmann E, Cramariuc D, Gerds E, et al. Impact of pressure recovery on echocardiographic assessment of asymptomatic aortic stenosis: a SEAS substudy. *J Am Coll Cardiol Img*. 2010; 3:555–562.
7. Rahimtoola SH. Determining that aortic valve stenosis is severe: back-to-the-future. *J Am Coll Cardiol Img*. 2010; 3:563–566.
8. Akins CW, Travis B, Yoganathan AP. Energy loss for evaluating heart valve performance. *J Thorac Cardiovasc Surg*. 2008; 136:820–833. [PubMed: 18954618]
9. Baumgartner H, Otto CM. Aortic stenosis severity: do we need a new concept? *J Am Coll Cardiol*. 2009; 54:1012–1013. [PubMed: 19729118]



10. Clark C. The fluid mechanics of aortic stenosis. I Unsteady flow experiments. *J Biomech.* 1976; 9:567–573. [PubMed: 965422]
11. Voelker W, Reul H, Stelzer T, Schmidt A, Karsch KR. Pressure recovery in aortic stenosis: an in vitro study in a pulsatile flow model. *J Am Coll Cardiol.* 1992; 20:1585–1593. [PubMed: 1452933]
12. Garcia D, Pibarot P, Dumesnil JG, Sakr F, Durand LG. Assessment of aortic valve stenosis severity: a new index based on the energy loss concept. *Circulation.* 2000; 101:765–761. [PubMed: 10683350]
13. Garcia D, Dumesnil JG, Durand LG, Kadem L, Pibarot P. Discrepancies between catheter and Doppler estimates of valve effective orifice area can be predicted from the pressure recovery phenomenon: practical implications with regard to quantification of aortic stenosis severity. *J Am Coll Cardiol.* 2003; 41:435–442. [PubMed: 12575972]
14. Baumgartner H, Steffenelli T, Niederberger J, Schima H, Maurer G. ‘Overestimation’ of catheter gradients by Doppler ultrasound in patients with aortic stenosis: a predictable manifestation of pressure recovery. *J Am Coll Cardiol.* 1999; 33:1655–1661. [PubMed: 10334438]
15. Clark C. Energy losses in flow through stenosed valves. *J Biomech.* 1979; 12:737–746. [PubMed: 489624]
16. Dyverfeldt P, Sigfridsson A, Kvitting JPE, Ebberts T. Quantification of intravoxel velocity standard deviation and turbulence intensity by generalizing phase-contrast MRI. *Magn Reson Med.* 2006; 56:850–858. [PubMed: 16958074]
17. Dyverfeldt P, Kvitting JPE, Sigfridsson A, Engvall J, Bolger AF, Ebberts T. Assessment of fluctuating velocities in disturbed cardiovascular blood flow: in vivo feasibility of generalized phase-contrast MRI. *J Magn Reson Imaging.* 2008; 28:655–653. [PubMed: 18777557]
18. Dyverfeldt P, Gardhagen R, Sigfridsson A, Karlsson M, Ebberts T. On MRI turbulence quantification. *Magn Reson Imaging.* 2009; 27:913–922. [PubMed: 19525079]
19. Elkins CJ, Alley MT, Saetran L, Eaton JK. Three-dimensional magnetic resonance velocimetry measurements of turbulence quantities in complex flow. *Exp Fluids.* 2009; 46:285–296.
20. Petersson S, Dyverfeldt P, Gardhagen R, Karlsson M, Ebberts T. Simulation of phase contrast MRI of turbulent flow. *Magn Reson Med.* 2010; 64:1039–1046. [PubMed: 20574963]
21. Arzani A, Dyverfeldt P, Ebberts T, Shadden SC. In vivo validation of numerical prediction for turbulence intensity in an aortic coarctation. *Ann Biomed Eng.* 2012; 40:860–870. [PubMed: 22016327]
22. Dyverfeldt P, Kvitting JPE, Carlhall CJ, et al. Hemodynamic aspects of mitral regurgitation assessed by generalized phase-contrast MRI. *J Magn Reson Imaging.* 2011; 33:582–588. [PubMed: 21563241]
23. Haimerl J, Freitag-Krikovic A, Rauch A, Sauer E. Quantification of aortic valve area and left ventricular muscle mass in healthy subjects and patients with symptomatic aortic valve stenosis by MRI. *Z Kardiol.* 2005; 94:173–181. [PubMed: 15747039]
24. Mathieu, J.; Scott, J. *An Introduction to Turbulent Flow.* Cambridge, UK: Cambridge University Press; 2000.
25. Gao JH, Gore JO. Turbulent flow effects on NMR imaging: measurement of turbulent intensity. *Med Phys.* 1991; 18:1045–1051. [PubMed: 1961145]
26. Baumgartner H, Hung J, Bermejo JB, et al. Echocardiographic assessment of valve stenosis: EAE/ASE recommendations for clinical practice. *Eur J Echo.* 2009; 10:1–25.
27. Pennel DJ, Sechtem UP, Higgins CB, et al. Clinical indications for cardiovascular magnetic resonance (CMR): Consensus Panel report. *J Cardiovasc Magn Reson.* 2004; 6:727–765. [PubMed: 15646878]
28. Hiratzka LF, Bakris GL, Beckman JA, et al. 2010 ACCF/AHA/AATS/ACR/ASA/SCA/SCAI/SIR/STS/SVM guidelines for the diagnosis and management of patients with thoracic aortic disease. A report of the American College of Cardiology Foundation/American Heart Association Task Force on Practice Guidelines, American Association for Thoracic Surgery, American College of Radiology, American Stroke Association, Society of Cardiovascular Anesthesiologists, Society for Cardiovascular Angiography and Interventions, Society of Interventional Radiology, Society of

- Thoracic Surgeons, and Society for Vascular Medicine. *J Am Coll Cardiol*. 2010; 55:e27–e129. [PubMed: 20359588]
29. van Pelt R, Nguyen H, ter Haar Romeny B, Vilanova A. Automated segmentation of blood-flow regions in large thoracic arteries using 3D-cine PC-MRI measurements. *Int J Comput Assist Radiol Surg*. 2012; 7:217–224. [PubMed: 21779767]
  30. VanAuker MD, Chandra M, Shirani J, Strom JA. Jet eccentricity: a misleading source of agreement between Doppler/catheter pressure gradients in aortic stenosis. *J Am Soc Echocardiogr*. 2001; 14:853–862. [PubMed: 11547270]
  31. Richards KE, Deserranno D, Donal E, Greenberg NL, Thomas JD, Garcia MJ. Influence of structural geometry on the severity of bicuspid aortic stenosis. *Am J Physiol Heart Circ Physiol*. 2004; 287:H1410–H1416. [PubMed: 15117719]
  32. Nerem RM, Seed WA. An in vivo study of aortic flow disturbances. *Cardiovasc Res*. 1972; 6:1–14. [PubMed: 5014275]
  33. Nygaard H, Hasenkam JM, Pedersen EM, Kim WY, Paulsen PK. A new perivascular multi-element pulsed Doppler ultrasound system for in vivo studies of velocity fields and turbulent stresses in large vessels. *Med Biol Eng Comp*. 1994; 32:55–62.
  34. Isaaq K, Bruntz JF, Da Costa A, et al. Noninvasive quantitation of blood flow turbulence in patients with aortic valve disease using online digital computer analysis of Doppler velocity data. *J Am Soc Echocardiogr*. 2003; 16:965–974. [PubMed: 12931109]
  35. Thorne ML, Rankin RN, Steinman DA, Holdsworth DW. In vivo Doppler ultrasound quantification of turbulence intensity using a high-pass frequency filter method. *Ultrasound Med Biol*. 2010; 36:761–771. [PubMed: 20381951]
  36. Tyszka JM, Laidlaw DH, Asa JW, Silverman JM. Three-dimensional, time-resolved (4D) relative pressure mapping using magnetic resonance imaging. *J Magn Reson Imaging*. 2000; 12:321–329. [PubMed: 10931596]
  37. Ebberts T, Wigstrom L, Bolger AF, Wranne B, Karlsson M. Noninvasive measurement of time-varying three-dimensional relative pressure fields within the human heart. *J Biomech Eng*. 2002; 124:288–293. [PubMed: 12071263]
  38. Binter C, Knobloch V, Manka R, Sigfridsson A, Kozerke S. Bayesian multipoint velocity encoding for concurrent flow and turbulence mapping. *Magn Reson Med*. 2012 Jun 14. [Epub ahead of print].
  39. Gu T, Korosec FR, Block WF, et al. PC VIPR: a high-speed 3D phase-contrast method for flow quantification and high-resolution angiography. *Am J Neuroradiol*. 2005; 26:743–749. [PubMed: 15814915]
  40. Sigfridsson A, Petersson S, Carlhall CJ, Ebberts T. Four-dimensional flow MRI using spiral acquisition. *Magn Reson Med*. 2012; 68:1065–1073. [PubMed: 22161650]

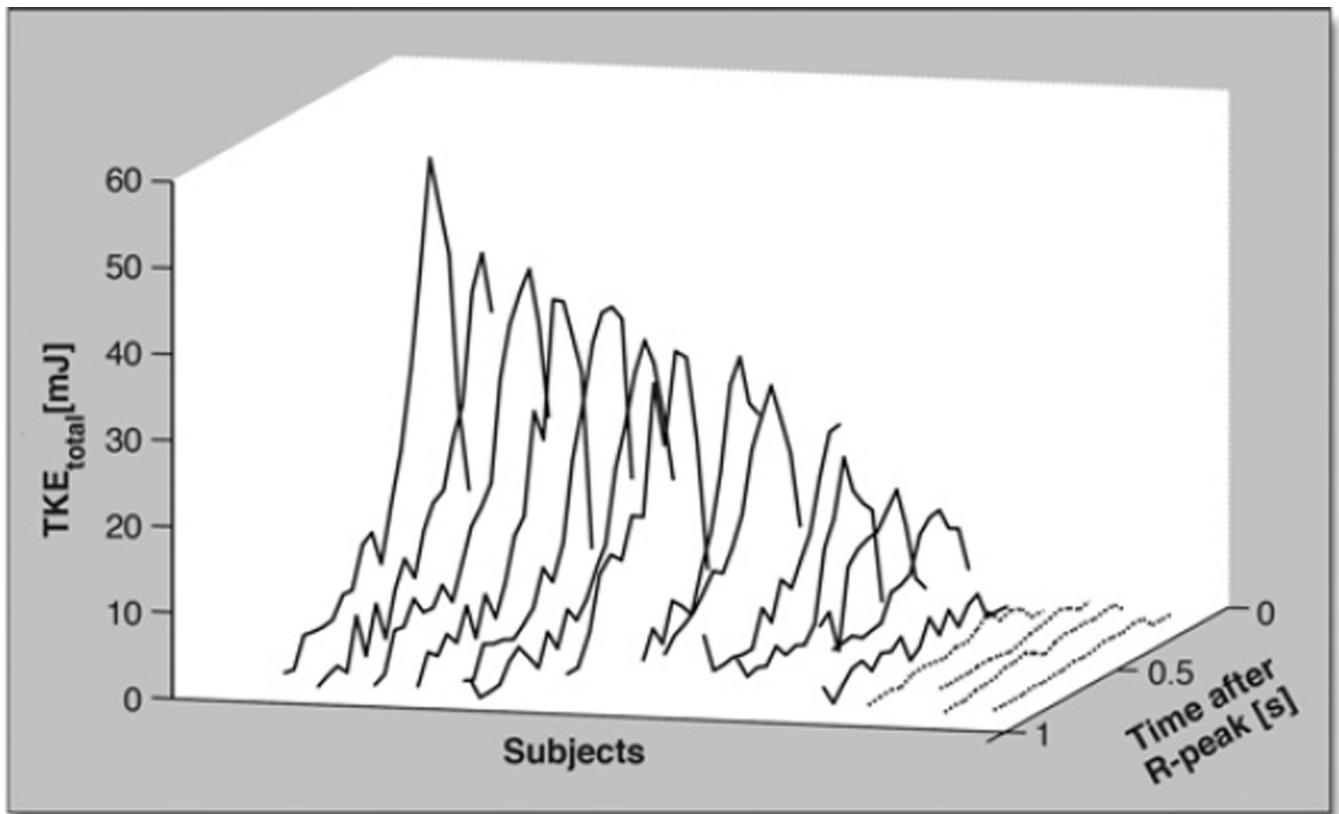


**Figure 1. Total TKE in the Ascending Aorta Over Time**

Plots of the total turbulent kinetic energy ( $TKE_{total}$ ) in the ascending aorta over time (time after R-peak) for normal volunteers (**dotted lines**) and patients with aortic stenosis (**solid lines**). Subjects are ordered according to peak total TKE along the second horizontal axis. The peak total TKE in the aortic stenosis patients was significantly higher than in the normal volunteers,  $p < 0.001$ .

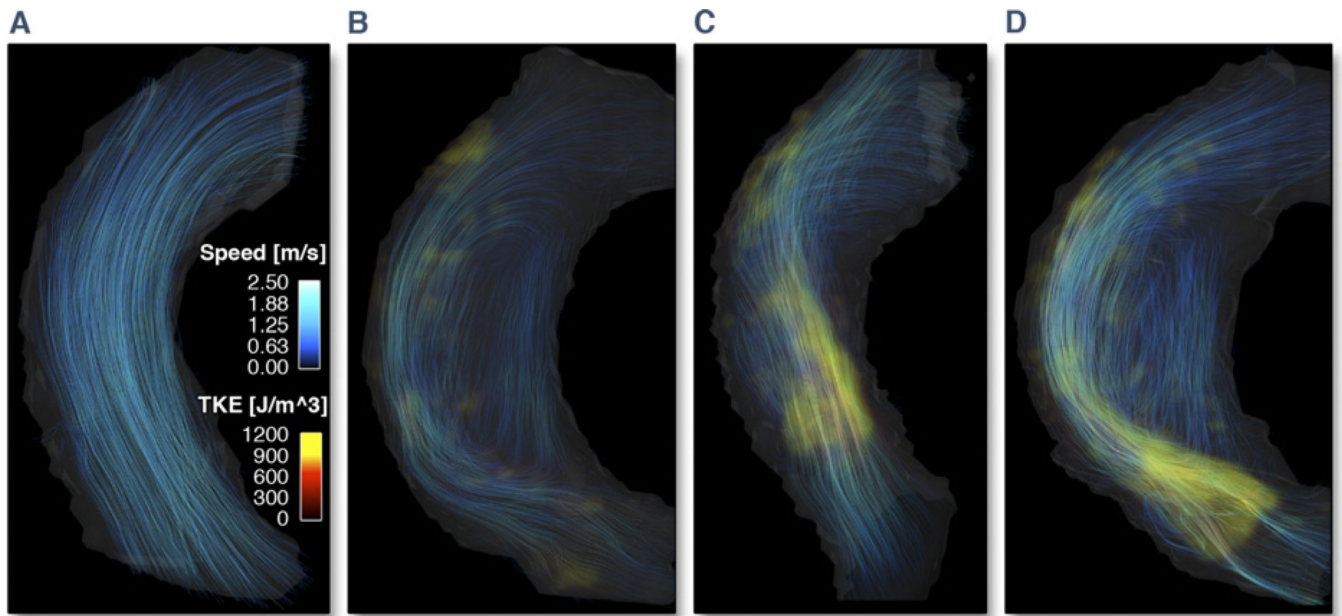


**Figure 2. Visualization of Flow Patterns and TKE**

Visualization of flow patterns and turbulent kinetic energy (TKE) in 1 normal volunteer and 3 patients with aortic stenosis. For each subject, volume renderings of TKE (red to yellow color scale) at the time point of peak total TKE have been combined with streamline visualization of the instantaneous velocity field at the time of peak velocity (blue color scale). Color settings were the same in all subjects.

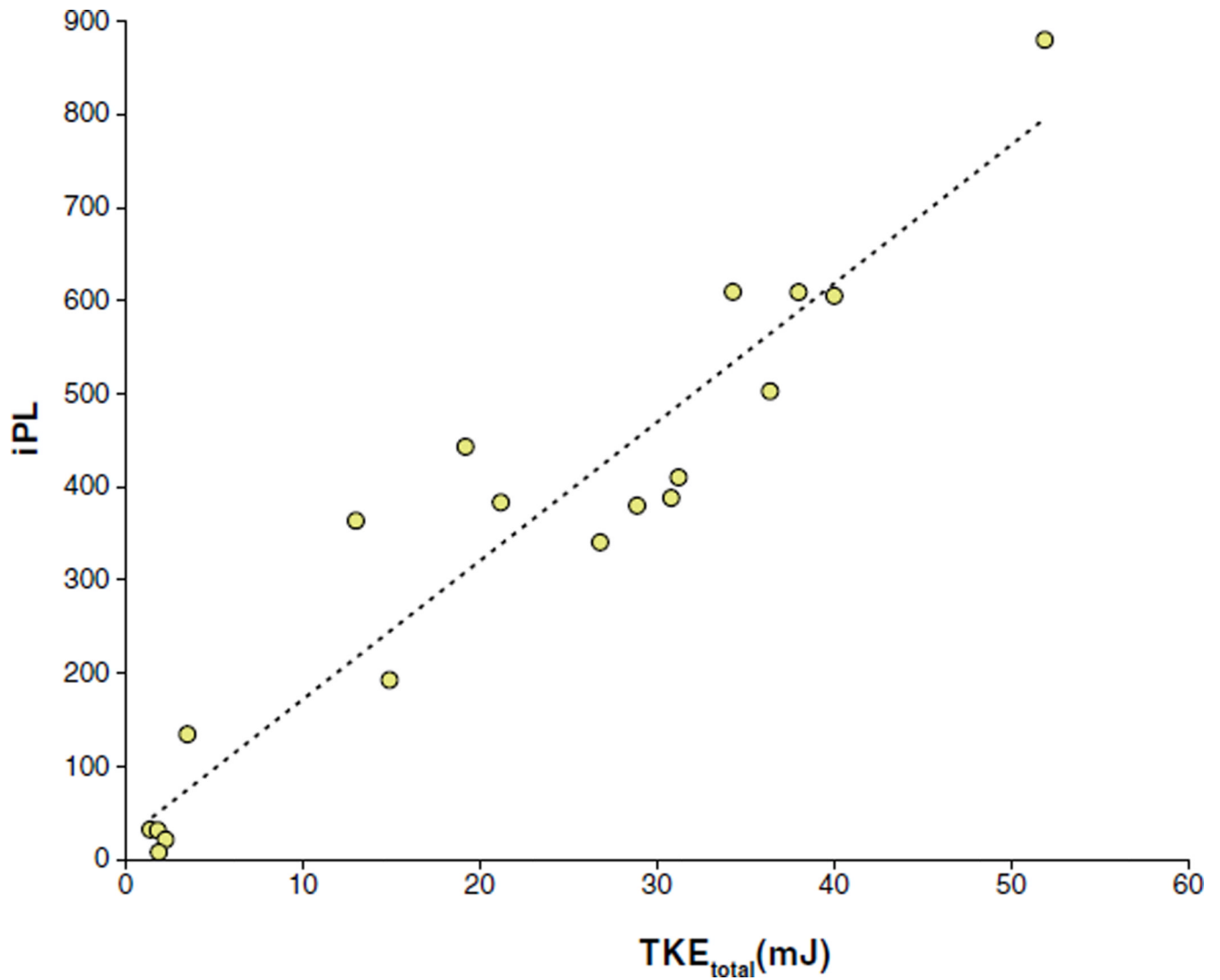


**Figure 3. Total TKE Versus Pressure Loss**

Total turbulent kinetic energy ( $TKE_{total}$ ) in the ascending aorta plotted against index pressure loss (iPL). The total TKE was obtained by integrating the TKE per unit volume across the entire ascending aorta. The iPL was calculated based on formulas validated by Garcia et al. (12,13). Total TKE was strongly correlated with iPL ( $R^2 = 0.91$ ).

Table 1

## Demographics and Clinical Data

Type	Age/Sex	Aortic Area at Sinotubular Junction (cm)	Aortic Valve Area (cm <sup>2</sup> )*	Max/Mean Pressure Gradient (mm Hg)†
Normal 1	24/M	5.7	4.4‡	n/a
Normal 2	36/M	6.2	4.2‡	n/a
Normal 3	32/F	4.5	3.2‡	n/a
Normal 4	28/F	4.3	3.6‡	n/a
Patient 1	90/M	6.6	0.4	215/136
Patient 2	71/M	7.1	0.9	62/38
Patient 3	51/M	14.5	0.9	70/38
Patient 4	69/M	6.2	0.82	65/39
Patient 5	72/M	8.0	1.52	62/33
Patient 6	78/M	7.5	0.64	75/48
Patient 7	69/M	9.6	0.95	52/35
Patient 8	67/M	5.7	0.78	114/71
Patient 9	64/M	9.1	1.0	56/30
Patient 10	79/M	8.1	0.79	112/68
Patient 11	74/M	9.1	0.63	56/30
Patient 12	80/M	8.5	0.5	91/57
Patient 13	55/M	11.9	4.7‡	n/a
Patient 14	57/F	8.5	3.6‡	n/a

\* Aortic valve area determined by the continuity equation method.

† Pressure gradients calculated from echocardiography velocity measurements using the Bernoulli equation. Pressure gradients were not available in subjects without aortic stenosis.

‡ Aortic valve area (AVA) in subjects without known aortic stenosis was estimated from the relationship:  $AVA = -2.64 + 0.04 \times (\text{height in cm}) - 0.47 \times w$  ( $w = 0$  for male,  $w = 1$  for female) (23).

n/a = not applicable.